Journal of Sustainable Metallurgy (2024) 10:296–310
https://doi.org/10.1007/s40831-024-00805-6

RESEARCH ARTICLE

Solar Assisted Production of $MgAl_2O_4$ from Bayer Process Electrofilter Fines as Source of Al_2O_3

Daniel Fernández-González[1] · Juan Piñuela-Noval[1] · Íñigo Ruiz-Bustinza[2] · Carmen González-Gasca[3] · Cristian Gómez-Rodríguez[4] · Linda Viviana García-Quiñonez[5] · Adolfo López-Liévano[4] · Adolfo Fernández[1] · Luis Felipe Verdeja[6]

Received: 27 June 2023 / Accepted: 11 February 2024 / Published online: 21 February 2024
© The Author(s) 2024

Abstract

Compared with conventional high-temperature methods based on electricity and fossil fuels, concentrated solar energy route offers distinct advantages in terms of mitigating emissions of contaminants and shortening processing times. Nevertheless, solar-based route also encounters challenges in producing significant quantities of materials, although the deployment of this technology is still conditioned by the limited investigation in the field. This study presents a novel high-temperature process based on solar energy to produce $MgAl_2O_4$ spinel, which employs as source of Al_2O_3 a waste from the aluminum industry: waste alumina fines from the Bayer process. First, mixtures were prepared by mechanical mixing in a molar ratio 1:1 in agreement with the MgO–Al_2O_3 binary phase diagram. Then, synthesis of the $MgAl_2O_4$ spinel was conducted by static experiments (5 min) with direct application of concentrated solar energy (1150 W/cm^2) at temperatures greatly exceeding 1800 °C as reported by ANSYS software. Wastes from three Bayer process factories were studied, which exhibited after the synthesis process a good crystallinity. The carbon dioxide emissions avoidance would range from the 200 to 500 tons of CO_2/year in the case of a small plant producing 1000 tons/year to 5000 to 12,000 tons of CO_2/year in the case of a commercial plant producing 25,000 tons/year, thus contributing to mitigate climate change. The proposed process might lead to smaller volume of wastes in the aluminum industry, while the $MgAl_2O_4$ may be used as raw material in the numerous fields based on the chemical, thermal, dielectric, mechanical and optical properties.

The contributing editor for this article was M. Akbar Rhamdhani.

✉ Daniel Fernández-González
d.fernandez@cinn.es

[1] Nanomaterials and Nanotechnology Research Center (CINN-CSIC), Universidad de Oviedo (UO), Principado de Asturias (PA), Avda. de la Vega, 4-6, 33940 El Entrego, Asturias, Spain

[2] Departamento de Ingeniería Geológica y Minera, Escuela Técnica Superior de Ingenieros de Minas y Energía, Universidad Politécnica de Madrid, 28003 Madrid, Spain

[3] Universidad UNIE, Calle Arapiles, 14, 28015 Madrid, Spain

[4] Departamento de Mecánica, Facultad de Ingeniería, Universidad Veracruzana, Campus Coatzacoalcos, Av. Universidad Km 7.5 Col. Santa Isabel, 96538 Coatzacoalcos, Veracruz, Mexico

[5] Centro de Investigación en Recursos Energéticos y Sustentables (CIRES), Universidad Veracruzana, Av. Universidad Veracruzana km 7.5, Col. Santa Isabel I, 96538 Coatzacoalcos, Veracruz, Mexico

[6] Departament of Materials Science and Metallurgical Engineering, School of Mines, Energy and Materials, Universidad de Oviedo, 33004 Oviedo, Uviéu, Asturias, Spain

Graphical Abstract

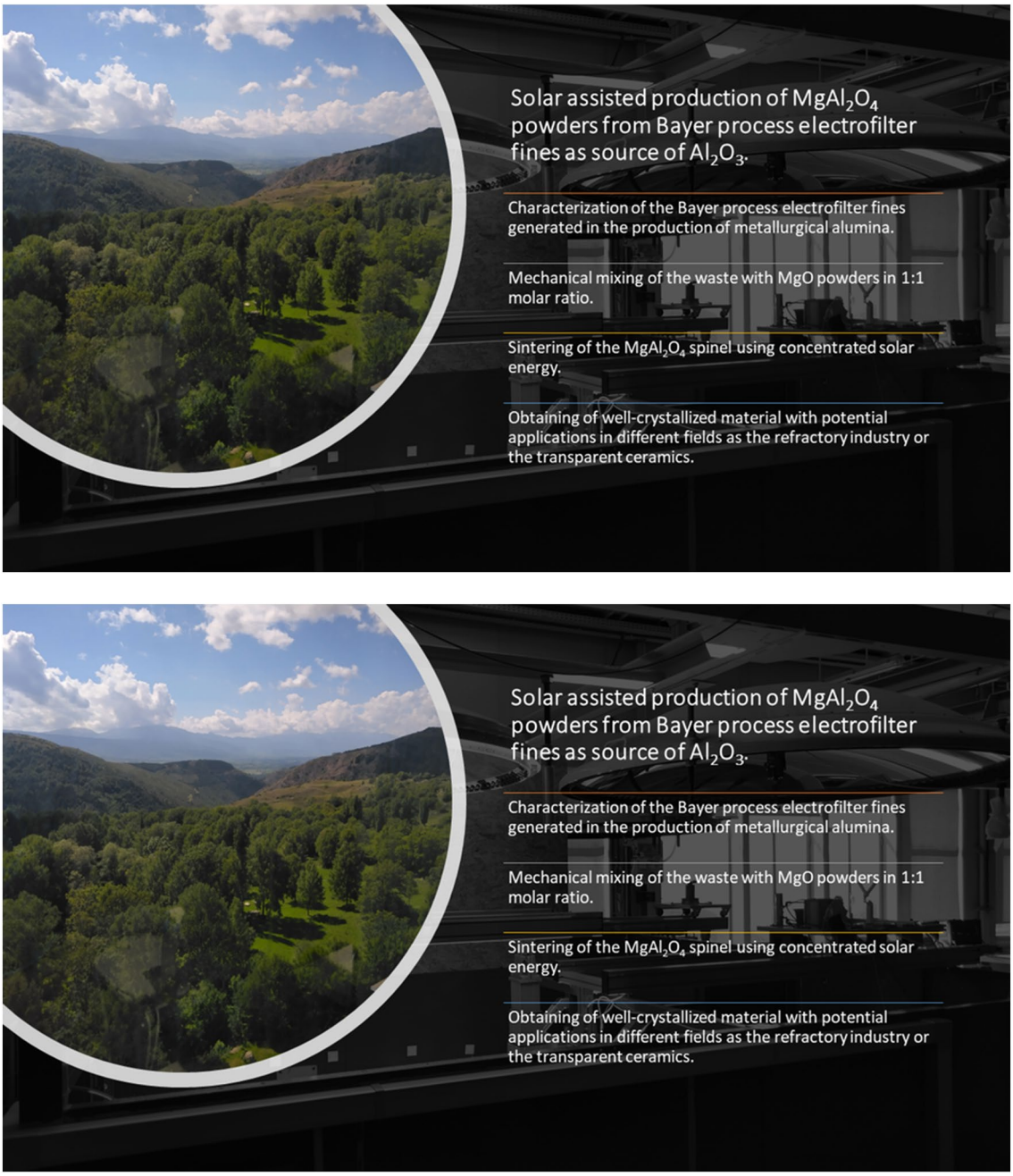

Keywords $MgAl_2O_4$ spinel · Concentrated solar energy · Metallurgy · Circular economy · Sustainability

Introduction

Aluminum industry, accounting for a smelter production of 68 Mt in 2021 according to the *United States Geological Survey*, is one of the most produced materials [1]. The production of aluminum is carried out by means of a process that involves two main stages, one, called Bayer process, which has as objective to produce alumina from bauxite

(consisting of mainly aluminum hydroxides with variable quantities of iron oxides, aluminum clays, kaolinite, and minor amounts of other oxides [2]) and the other, called Hall-Hérault process, which aims at producing aluminum by electrolysis in a molten electrolyte of cryolite. Focusing on the Bayer process, it involves several stages that include the pressure leaching of bauxite ore with aqueous soda solution, precipitation of aluminum hydrate (bayerite) from clean solution and calcination of the hydrate to produce alumina, which is later employed as raw material in the Hall-Hérault process.

Electrofilter fines are a residue generated in this process in quantities of around 5–8% of the final alumina product (approximately 80,000–100000 tons for a 1.2 Mt alumina plants [3]). It consists of a mixture of different aluminas and alumina hydrates with small particle size that are collected as a residue in the electrofilter equipment. Different studies were conducted to find an application or extract valuable components from the electrofilter powders generated in the Bayer process, although there is still not any process with a massive implementation in the industry. This way, Bayer process electrofilter fines have been used in the production of ceramic materials as Tutic and collaborators, which obtained mullite ceramics from Bayer electrofilter fines and low kaolinite clay [4], and Sancho-Gorostiaga and others [5], which proposed the utilization of this waste in the manufacture of high temperature structural insulators. Other researchers tried to collect components from the residue as Okudan and collaborators, which attempted to recover gallium and aluminum [6]. For their part, Ayala and Pérez [7] investigated the removal of Se(VI) from aqueous solution using Bayer process electrofilter fines. Finally, other research in this line was conducted by Sancho et al. [8] and Ayala et al. [9], which recycled electrofilter fines as aluminum sulphate for water coagulant uses, Sancho and co-authors [3], which suggested that fines could be recycled as industrial quality aluminum sulphate, alums, and abrasives, and Sancho-Gorostiaga and colleagues [10], which investigated about the removal of copper from aqueous solutions using Bayer process electrofilter fines.

Solar energy, when it is adequately concentrated, offers enormous possibilities in metallurgy and materials science [11]. A recent state-of-the-art review of Fernández-González [12] makes a deep literature survey of the applications of solar energy in the field of materials. Our research group has made intensive work in the application of concentrated solar energy in the synthesis of materials: silicon-calcium [13], where the synthesis of this energy-intensive alloy used in deoxidizing of steels was attempted from mixtures of CaO and Si to avoid carbon dioxide emissions and energy costs, although it was produced in minor quantities associated to the atmosphere of the process; silicon-manganese [14], where the synthesis of this alloy typically used in the production of steels was achieved from mixtures of manganese (IV) oxide and silicon; calcium aluminate cements [15], where the most relevant result was the synthesis of main components of the high alumina (> 75%) calcium aluminate cements using limestone as source of CaO for the process; operations in the field of iron and steels [16], where metallic iron was obtained from iron ore sinter fines reduced by coke with the heat support of solar energy; and, zirconia [17], which was obtained by solar thermal decomposition of zirconium silicate sand and subsequent separation of the ZrO_2 by pressure leaching with NaOH of the silica. Focusing on the aluminum field, solar energy has been applied to reduce the environmental impact by using a zero-CO_2 energy. First investigations in this line can be attributed to J. P. Murray [18], who proposed the direct reduction of Al_2O_3 to aluminum or aluminum–silicon alloy or reduction to AlN or Al_2S_3 that could be more easily electrolyzed with non-consumable electrodes. Several studies were conducted from that moment in line with the production of aluminum by carbothermal reduction with more or less success in the obtaining of metallic aluminum [19–24]. Alternatively, Lytvynenko [25] proposed the utilization of solar energy in the obtaining of aluminum by electrolysis through the Hall-Herault's process using the current of a solar battery and employing solar radiation to heat the cell. In the same line, other researchers proposed the calcination of the aluminum hydroxide to obtain alumina to feed the cell for the electrolysis of aluminum using solar energy [26, 27].

Nevertheless, apart from the potential application of solar energy in the synthesis of materials, there is a growing interest in its application to recycle or recover valuable components from industrial wastes, for instance in the extraction of copper and iron from copper slags [28] or iron from basic oxygen furnace slags [29], due to the possibility of heating without releasing pollutant. The research in this field focuses not only on the recovery of metals from slags but in the immobilization of contaminants, as filter dusts [30, 31] or soil and mine waste samples containing mercury [32–35]. Anyway, the application of solar energy in recycling or recovering metals is the most important line due to the lower temperatures required in the case of operating with them whether compared with ceramics. Therefore, other researchers aimed at recovering metals (Zn, Fe, Pb and Cu) from electric arc furnace dust (EAFD) and automobile shredder residue (ASR) [36, 37], extracting zinc from Waelsz oxide produced during the recycling of galvanized steels [38] or used solar energy to melt aluminum scrap [39–42]. Nevertheless, as a consequence of the high temperatures that can be reached with the competition of solar energy (above 2500 °C [11, 12]) researchers have also attempted to recycle aluminum oxides. This way, studies guided by Padilla and collaborators [43] in the field of

aluminum waste were conducted to obtain alumina from boehmite prepared by sol–gel process from an aluminum waste that proceeded from the fine suction system used in the aluminum slag milling operation. The same authors, Padilla and researchers [44], attempted the production glasses also from aluminum wastes, which consisted in a powdered solid trapped in filter sleeves during the slag milling process of the aluminum tertiary industry. Apart from the aluminum residue, these researchers employed other wastes as eggshells and mussel shells as sources of calcium for the glass.

Magnesium aluminate compound is a spinel that is gaining interest in different applications due to the excellent chemical, thermal, dielectric, mechanical and optical properties [45]. Nevertheless, magnesium aluminate spinel is an excellent refractory oxide of great importance as structural ceramic due to the physical, chemical, and thermal properties at normal and elevated temperatures [46]. Different methods can be used to obtain the $MgAl_2O_4$ spinel. These methods include sol–gel reaction [47], gelatin method [48], metal-chitosan complexation [49], thermal decomposition [50], hydrothermal [51], high-energy ball mill [52], microwave assisted combustion [53], organic precursor combustion [54], sonochemical [55], spray pyrolysis [56], spray drying [57], among other processes [47]. Anyway, the most habitual technique to synthesize this spinel is the solid-state reaction from powders of MgO and Al_2O_3, although the process has several disadvantages including long processing times, need for repetition of several calcination stages, requirement of high temperatures for sintering [46]. Some of these issues might be solved with the application of concentrated solar energy. For that reason, this manuscript proposes a novel method to synthesize $MgAl_2O_4$ from Bayer process electrofilter fines at laboratory scale using concentrated solar energy as potential route to reduce carbon dioxide emissions.

Materials and Methods

Raw Materials

Three different Bayer Process Electrofilter Fines (BPEFs) were used as source of Al_2O_3 in the obtaining of the $MgAl_2O_4$ spinel, while the MgO was provided by an industrial supplier. The BPEFs were generated in Bayer process plants located in three different countries: Canada, Ireland, and Spain. The chemical composition was determined by inductively coupled plasma mass spectrometry, while carbon and sulphur contents were obtained by combustion with the equipment CS800 Eltra. Results for the BPEFs are collected in Table 1. The structure of the BPEFs was analyzed by X-ray diffraction, which reported different types of alumina (mainly α- and γ-alumina, whose content was determined by means of the area below the X-ray diffraction pattern) with certain amounts of gibbsite ($Al(OH)_3$). The carbon content gives a characteristic grey color to the sample. Mean particle size (d_{50}) was determined by photosedimentometer Lumosed equipment. The water content in the samples is represented by the Moisture on Ignition (MOI, mass losses when heating the sample up to 550 °C for 2 h) and Lost on Ignition (LOI, mass losses when heating the sample up to 900 °C for 2 h). Additionally, the content in aluminum trihydrate (gibbsite) was determined by thermal analysis technique (Mettler-Toledo DSC822e), under a nitrogen atmosphere (50 ml/min) and at a heating rate of 5 °C/min to determine the endothermic peak corresponding to the hydrate water loss, where patterns with variable contents in gibbsite (from 0.5 to 50%) were employed to obtain the calibration line. This parameter is important because gibbsite is also a source of Al_2O_3 for the spinel although before the reaction with the MgO, the aluminum trihydrate decomposes into Al_2O_3 and H_2O, which leads to problems of decrepitation. Numerical values of the characteristics of the BPEFs are collected in Table 2.

Table 1 Composition of the BPEFs of the three Bayer process factories

(%)	Al_2O_3	Na_2O	SiO_2	Fe_2O_3	CaO	K_2O	TiO_2	MgO	Ga_2O_3	C	S
Canada	87	0.70	< 0.04	< 0.04	0.03	< 0.04	< 0.01	< 0.01	0.008	0.08	0.02
Ireland	92	0.46	< 0.04	< 0.04	0.02	< 0.04	< 0.01	< 0.01	0.012	0.14	0.02
Spain	91	0.67	< 0.04	< 0.04	0.01	< 0.04	< 0.01	< 0.01	0.012	0.14	0.02

Table 2 Characteristics of the BPEFs of the three Bayer process factories

	MOI (%)	LOI (%)	α-Alumina	γ-Alumina	Gibbsite (%)	d_{50} (μm)
Canada	10.0	2.30	19.0	49.0	29.0	7.8
Ireland	5.3	1.60	17.0	65.5	14.5	5.3
Spain	6.6	0.7	33.0	32.2	18.0	8.7

Magnesia was provided by Grupo Peñoles (Mexico). The chemical composition of the magnesia was determined by X-ray fluorescence spectrometry. Results are collected in Table 3.

Methods

Experiments were carried out in a vertical axis solar furnace located in Font Roméu-Odeillo-Via (France), which belongs to the PROMES-CNRS (PROcédés Matériaux et Energie Solaire-Centre National de la Recherche Scientifique). It consisted in a 1.5 m in diameter parabolic concentrator that is illuminated with flat heliostat, which has a sun tracking system. This way, a maximum concentration ratio of 15,000 in a focal point of ≤ 1.5 cm is achieved. This means that the maximum concentrated power would be 900 W for a 1000 W/m^2 DNI (Direct Normal Irradiation), achieved with clean skies and parabolic concentrator. Experiments were conducted under a glass hood to avoid the deterioration of the parabolic concentrator with the powders that could leave the sample. Besides, air suction was applied to avoid the deposition of the powders in the glass hood, which would have been detrimental to the process. A scheme of the process appears represented in the Fig. 1.

The route chosen to manufacture the $MgAl_2O_4$ spinel was the solid-state reaction. Mixtures were prepared in a 1:1 molar ration according to the following chemical reaction:

$$MgO\ (s) + Al_2O_3(s) \rightarrow MgAl_2O_4(s) \quad (1)$$

which according to the binary phase diagram MgO-Al_2O_3 is in the stoichiometric spinel zone. Sintering zone, according to Sarkar and Banerjee [58], occurs in the temperature range 1550–1650 °C, although the formation of the spinel occurs also at greater temperatures as it appears in the phase diagram.

The temperature of the spot generated by the concentrated solar energy was determined by finite element method-based software ANSYS. The dimensions of the crucible were 19.55 mm in inner diameter, thickness of 3.28 mm and height of 25.4 mm, manufactured in alumina. The crucible was filled with a mixture of powders of Al_2O_3 and MgO in the proportion 1:1 molar. The following properties were considered for the thermal simulation: density, thermal conductivity, and specific heat of the different materials in agreement with the proportions. It is possible to see in Fig. 2a the scheme of the process with the dimensions used in the calculations. The analysis was carried out in a transient thermal module using the ANSYS Workbench application. To ensure the reliability of simulation results, a finite element mesh convergence analysis was conducted. This entailed progressively refining the finite element mesh from a coarse (Fig. 2b (1) coarse mesh) to a finer resolution (Fig. 2b (2) refine mesh), resulting in an increased number of elements/nodes. Throughout this iterative process, temperature variations were monitored until reaching a point where the variations became negligible. Additionally, a finer mesh refinement was implemented specifically in the central region of the specimen, where the energy beam impacts. On another note, Fig. 2c and d show the simulations conducted with the software ANSYS for different spot size and, therefore, energy density. The dwell time was in both situations 5 min, with 5 min of cooling. Figure 2c shows the simulation done with a beam of 10 mm in diameter, which involves 1150 W/cm^2 of energy density. This situation reported a maximum temperature of 1944 °C. On the other hand, Fig. 2d represents the simulation done with a beam of 15 mm in diameter, which involves 550 W/cm^2 of energy density. This scenario gave a maximum temperature of 1676 °C.

Mathematical simulations carried out are useful to know the approximate temperature of the spot, but they are not adequate to understand the complete process. This way, mathematical simulations report that the temperature in the spot is sufficiently high to synthesize the $MgAl_2O_4$ spinel. The simulations did not consider the consumption of the material as the process advances, it is necessary to consider that the final volume is 1/3 of the initial (the reasons are: powders manually compacted and sinter during the process, decrepitation, water losses, and flying of fines due to the air currents inside of the glass chamber). It is necessary to introduce in this point the thermocouple control. The thermocouple can be used to control the advance of the process as when the temperature starts to fall in the point where it is located (Fig. 1b), it is possible to assume that radiation is not producing any effect on the sample. Figure 3 serves as an example of the thermocouple measurements. The utilization of thermocouples inside of the sample is not a suitable strategy because they move and melt during the process.

There is not a control of the radiation applied to the sample (in other solar furnaces it is possible to employ a shutter to control the percentage of incident radiation that is applied to the sample). Within this line incident radiation during the experiments presented in this manuscript exceeded 950 W/m^2, which indicates that a power of around 0.9 kW was applied on a surface < 1.5 cm in diameter.

The duration of the treatment was considered a crucial factor in the manufacture of the $MgAl_2O_4$ spinel. Within this context, each experiment lasted 5 min. If

Table 3 Characteristics of the MgO

MgO (%)	CaO (%)	SiO_2 (%)	Al_2O_3 (%)	Fe_2O_3 (%)	B_2O_3 (%)	d_{50} (μm)
98.5	1	0.2	0.15	0.13	0.01	< 45

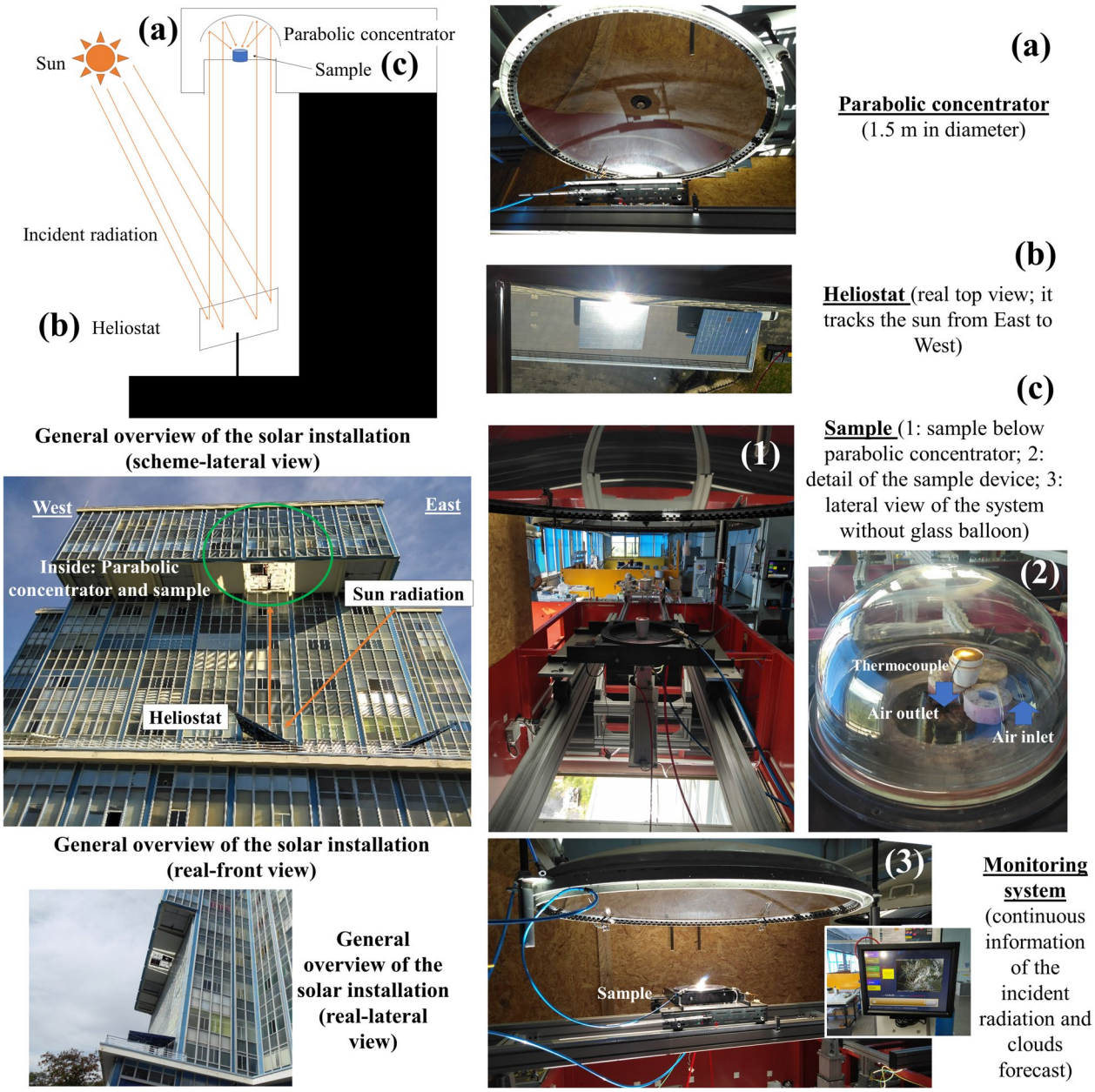

Fig. 1 Scheme and real images of the installation and devices used in the experimental work

the operations of charging the crucible and cooling are included, the process would last approximately 20 min in total. It is necessary to consider that the process presented in this manuscript is based on the direct application of the solar radiation to the sample. Nevertheless, there are technologies to directly process powders in solar furnaces [12]. This might be following step that should be studied in the scalation of this technology up to industrial scale, as the direct processing of powders would significantly increase the productivity of the process.

Results and Discussion

Mass Differences

Table 4 collects the weight losses produced during the experiments, which are consequence of several reasons discussed in the following lines.

Water: this is the main reason of the mass differences resulted from the treatment of the samples with concentrated solar energy. Aluminum industry residue (BPEF)

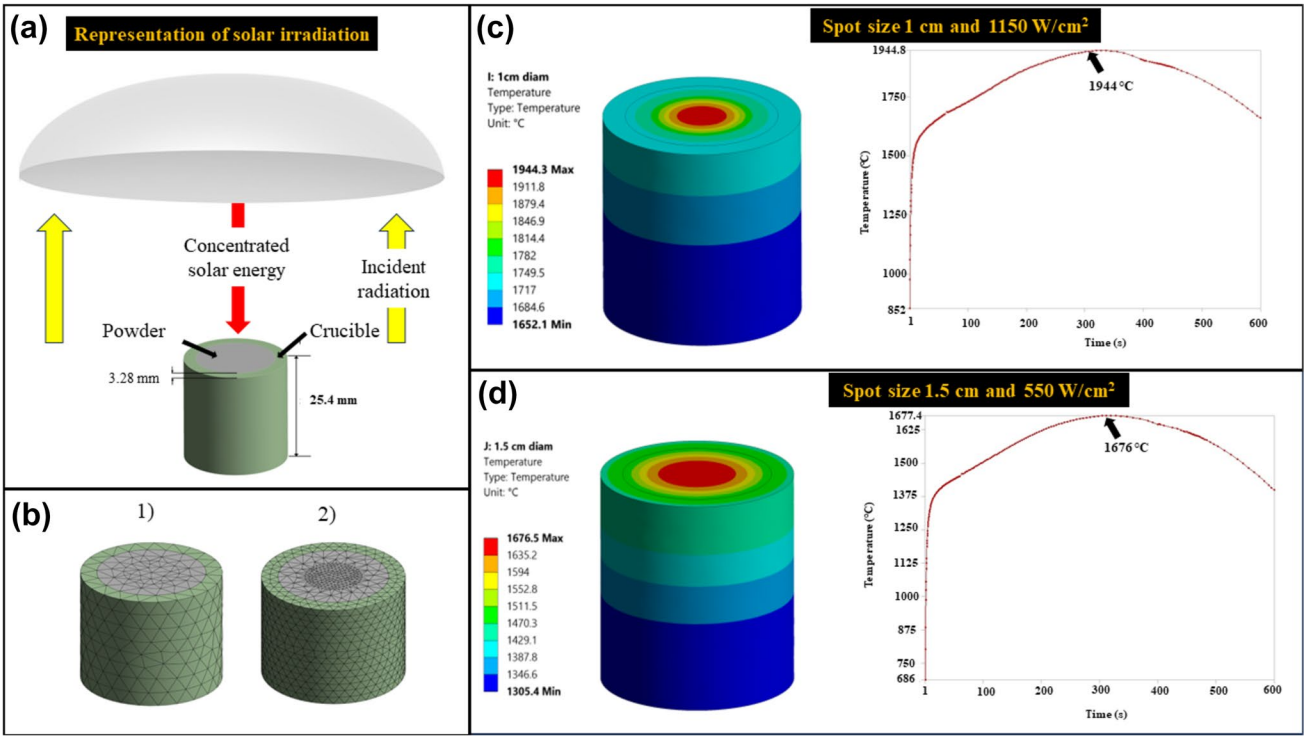

Fig. 2 **a** representation of solar irradiation, **b** meshing of the crucible and charge **c** simulation carried out with a spot size of 1 cm and 1150 W/cm^2 and **d** simulation carried out with a spot size of 1.5 cm and 550 W/cm^2

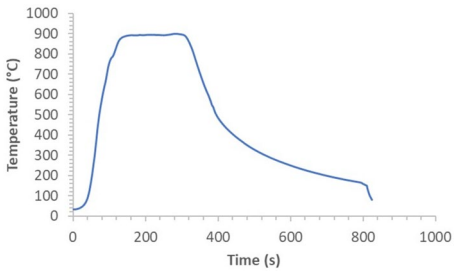

Fig. 3 Thermocouple measurement, located in the point indicated in the Fig. 1B

was not subjected to any previous treatment, and it contains certain quantity of physical water resulted from the storage outdoors. This involves that moisture depending on the γ-alumina content was: 0.9% in Canada BPEFs, 2.6% in Ireland BPEFs and 0.4% in Spain BPEFs. Additionally, there is certain quantity of chemical water since the residue contains aluminum hydroxide that decomposes at temperatures of around 550 °C according to the reaction 2.

$$2Al(OH)_3(s) \rightarrow Al_2O_3(s) + 3H_2O\,(g) \quad (2)$$

It is necessary to consider MOI measurements for Canada BPEFs were as high as 10%, while those corresponding to

Table 4 Weight losses produced during the treatment with concentrated solar energy

	Initial weight (g)	Final weight (g)	Mass losses (%)
Canada 1	4.8	2.8	41.7
Canada 2	3.3	2	39.4
Canada 3	3	2	33.0
Ireland 1	3.2	2.4	25.0
Ireland 2	2.8	2.2	21.4
Ireland 3	2.9	2.3	20.7
Spain 1	3	2	33.0
Spain 2	3.8	2.7	29.0
Spain 3	3.4	2.8	17.6

the BPEFs of Ireland and Spain were 5.3% and 6.6%, in agreement with the greater or lower gibbsite content. Average mass losses were 38% in the case of Canada BPEFs, 22.4% in the case of Ireland BPEFs and 26.5% in the case of Spanish BPEFs. Therefore, losses are directly related to the gibbsite content in the residue, which is reasonable considering the water content in the hydroxide.

Volatile matter: the residue contains alkali metals, mainly Na_2O, which according to the literature can evaporate at temperatures in the range 1500–1560 °C [59]. These authors

indicate that the presence of Al_2O_3 promote the evaporation ratio (MgO also plays the same role, but it only slightly enhances the evaporation ratio). Carbon, which is in minor contents but gives the characteristic grey color to the mixture, is also susceptible of being burned at the temperatures of the treatment.

Flying powders and decrepitation: The presence of an air current inside of the glass balloon leads to powder flying at the beginning of the treatment of the sample with concentrated solar energy. This problem is also observed in the case of operating without glass hood. Nevertheless, one of the reasons of the mass losses is the decrepitation produced due to the fast-heating rate and the presence of water and hydrated compounds in the sample. It is necessary to consider that powders are very fine, $d_{50} < 45$ µm, which suggests that green compacts could be a suitable option to process these materials or employ a reactor like those proposed by other authors in the case limestone calcination [60] or ZnO-Zn loop [61].

Quantitatively, mass losses associated with water (moisture + LOI + MOI, included the dehydration of the gibbsite) account for 28.50%, with chemical reactions (volatile compounds + carbon combustion) are < 2% and with projections, decrepitation and flying powders are 69.5%. The presence of impurities might play the role of fluxes, for instance sodium oxide is a common flux, but considering the excesses of energy employed in the proposed process the influence of the impurities in the reduction of the temperature is not relevant.

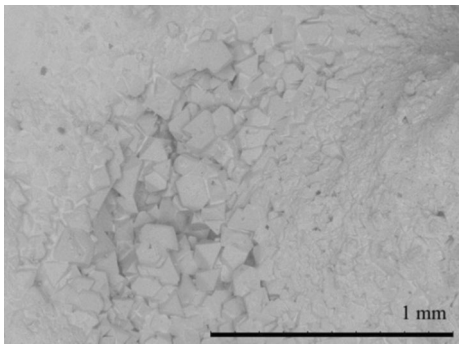

Fig. 4 Bulk $MgAl_2O_4$ spinel sample obtained after the treatment with concentrated solar energy

Microstructural Characteristics

The product at the end of the treatment consisted in bulk material as it is showed in Fig. 4. This sample may be grounded and milled to the desired grain size for further applications. Likewise, other alternative may be the obtaining of sintered discs of $MgAl_2O_4$ spinel, or the direct processing of powders as it was already anticipated. Despite the final product is obtained as a bulk material, it is crystalline as it is later reported in the X-ray diffraction analyses. In fact, if the Fig. 4 is observed, it is possible to check that crystals of $MgAl_2O_4$ spinel are obtained at macroscopic scale. Figure 5a and b show images of the $MgAl_2O_4$ spinel crystals at greater magnification.

Specimens were characterized by X-ray diffraction technique. This technique illustrates that the product obtained after the treatment is really $MgAl_2O_4$ spinel with the suitable crystallinity. X-ray diffraction patterns are collected in Fig. 6 for the three $MgAl_2O_4$ spinel prepared with the three BPEFs: Fig. 6a, $MgAl_2O_4$ spinel with Canadian BPEFs; Fig. 6b, $MgAl_2O_4$ spinel with Irish BPEFs; and Fig. 6c, $MgAl_2O_4$ spinel with Spanish BPEFs.

X-ray diffraction patterns report well crystallized specimens with no traces of the starting raw materials, which indicates that the treatment with concentrated solar energy allowed to obtain the $MgAl_2O_4$ spinel, as it was expected from the phase diagram. Amorphous content in samples is: Canadian 5.4% ± 2.0, Irish 5.0% ± 1.9, and Spanish 5.6% ± 2.0, determined with the XPowder Software.

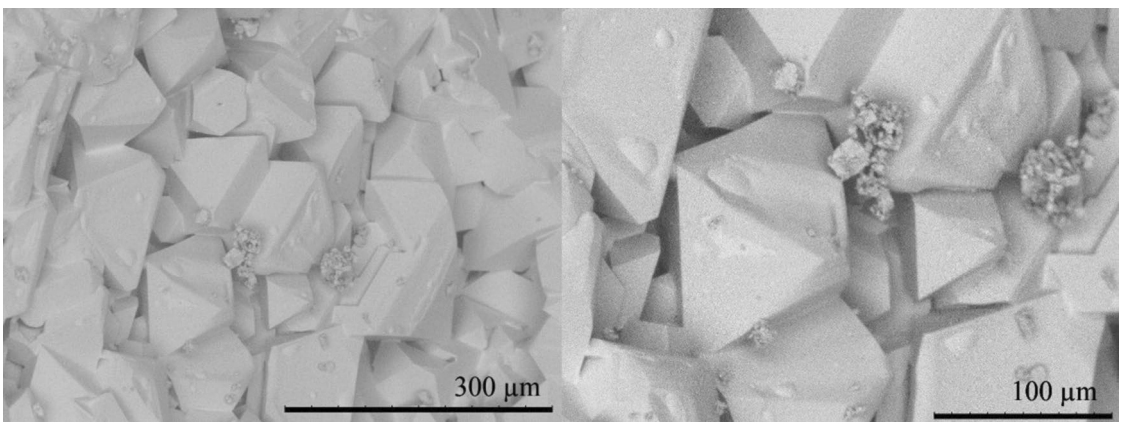

Fig. 5 Details of $MgAl_2O_4$ spinel crystals

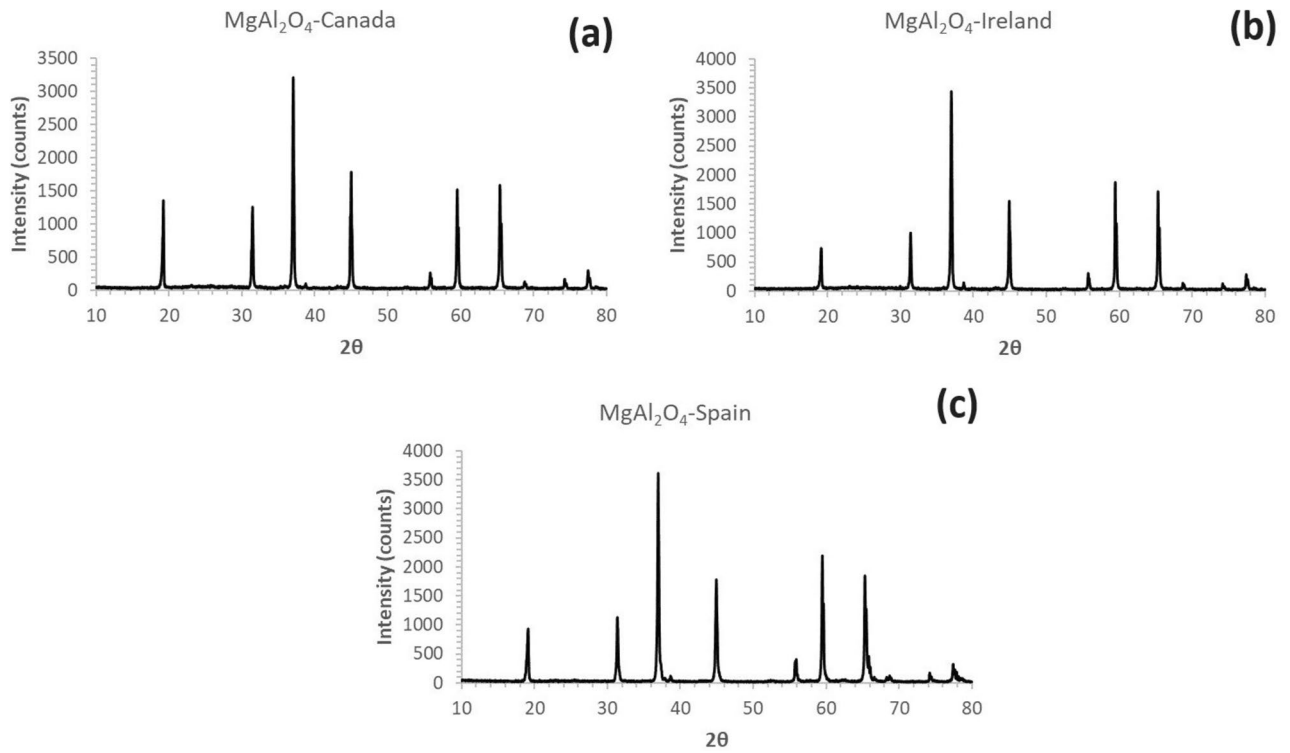

Fig. 6 X-ray diffraction of $MgAl_2O_4$ spinel using **a** Canadian BPEFs, **b** Irish BPEFs, and **c** Spanish BPEFs

Figure 7 collects the X-ray diffraction patterns of various $MgAl_2O_4$ spinels, either found in the nature as minerals or synthesized in laboratories. The form of the diffractograms analogous in the form to that obtained with the competition of concentrated solar energy.

The X-ray diffraction parameters 2θ and d-spacing for the hkl planes are compared with those of the reference work of Paterson and researchers [62], and some other $MgAl_2O_4$ spinels found in the nature and synthesized in laboratory. This allows checking the quality of the obtained $MgAl_2O_4$ spinel. Results are collected in Table 5 for the positions of the peaks and Table 6 for the d-spacing of the hkl planes. There is significant approximation of the values of the solar synthesized $MgAl_2O_4$ spinel to those obtained by Paterson and co-authors [58], as well as to those found in the nature and, particularly to that synthesized in the laboratory, which is evidence of the well crystallization of the spinel obtained by means of concentrated solar energy using Bayer process electrofilter fines as source of alumina.

Energy Efficiency and Technical Feasibility

Solar energy is a powerful source of heat that can be used in the obtaining of energy intensive products without carbon dioxide release in short times derived from the fast heating and cooling rates, as it is possible to see in Figs. 2 and 3. The synthesis of $MgAl_2O_4$ spinel is an energy intensive process, which is usually carried out at temperatures within 1550 and 1650 °C, although it is possible to obtain it at lower temperatures (> 550 °C) with prolongated permanence at these temperatures (> 4 h). Ping et al. remarked that the time for the synthesis of the $MgAl_2O_4$ spinel is a relevant issue [46]. Within this line, routes proposed at laboratory scale by different authors are still time consuming and, therefore, synthesizing the spinel in short times is still a challenge. The low temperature synthesis by sol–gel process proposed by Pei and researchers [64] lasts at least 6 h, the process of modified sol–gel process proposed by Sanjabi and Obeydavi [65] also lasted at least 6 h, Meng and colleagues [66] indicate that their process took about 3 h. On the other hand, Bocanegra and co-authors [67] proposed different routes of synthesis that took > 36 h (ceramic method), > 48 h (mechanomechanical synthesis) and > 30 h (co-precipitation). In the field of mechanomechanical synthesis too, Kong et al. [50] required more than 14 h to sinter $MgAl_2O_4$ spinel, with 12 h of milling in planetary ball milling and 2 h of sintering in furnace. Zhang in the hydrothermal route, required more than 31 h to synthesize the spinel [49]. On the other hand, Bai and researchers [68] employed more than 4 h in the combustion method. Citric acid–ethylene glycol route was used for the synthesis of $MgAl_2O_4$ nano-powder, involving a synthesis time of 40 h [69]. The solar process could be competitive with microwave sintering, as irradiation lasts less than 1 h [51], although the process has the inconvenient

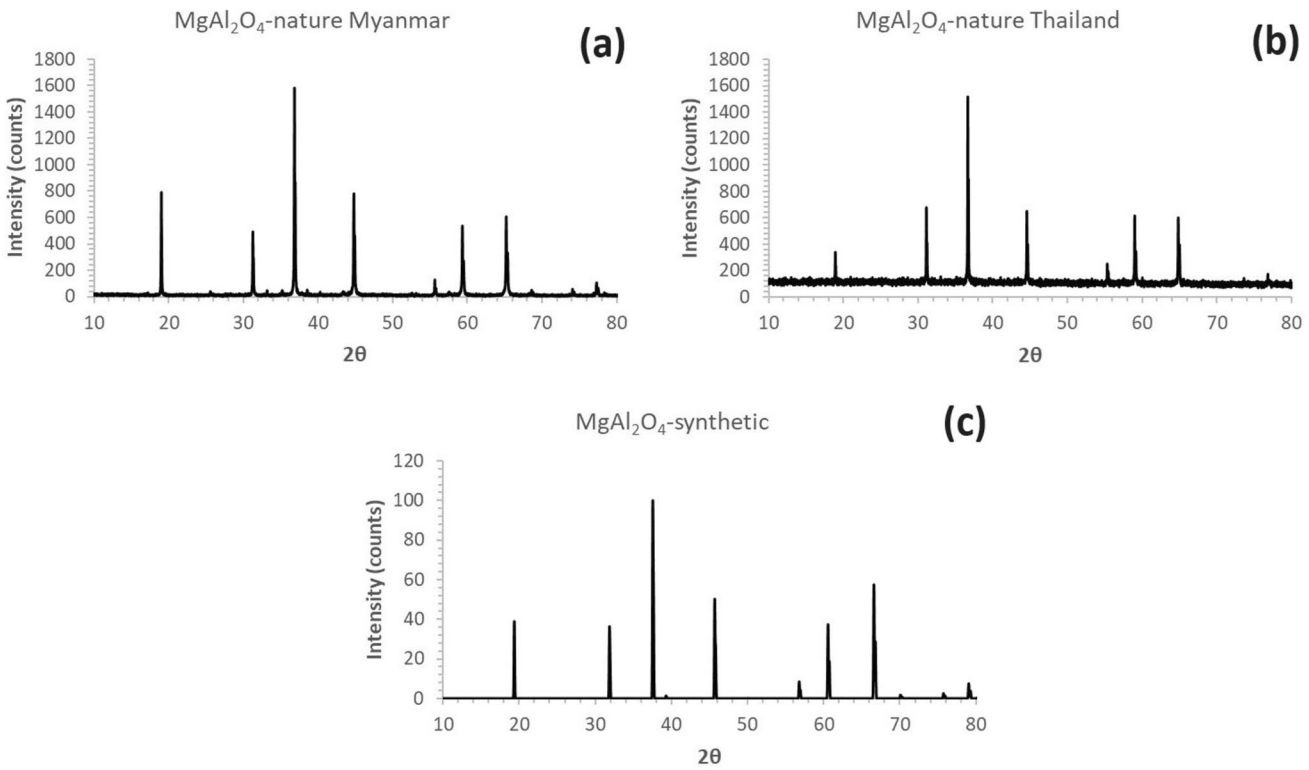

Fig. 7 X-ray diffraction of $MgAl_2O_4$ spinel found in nature (Myanmar) (**a**), nature (Thailand) (**b**), and synthesized in laboratory (**c**)

Table 5 Position of the peaks in the X-ray diffraction pattern of solar $MgAl_2O_4$ spinel compared with those obtained by Paterson et al., (1991) [58] and some other spinels either found in the nature or synthesized in the laboratory

	$MgAl_2O_4$ -from Pein Pyit, Mogok, Myanmmar (natural) [58]	$MgAl_2O_4$ -from Bo Phloi, Kanchoutabori Province, Thailand (natural) [63]	$MgAl_2O_4$—(synthetic) [58]	$MgAl_2O_4$ -Canadian BPEFs	$MgAl_2O_4$ -Irish BPEFs	$MgAl_2O_4$ -Spanish BPEFs
2θ	19.02		19.37	19.183	19.103	19.083
	31.28	31.11	31.89	31.446	31.386	31.366
	36.85	36.65	37.58	37.048	36.968	36.968
	38.55		39.32		38.688	
	44.81	44.56	45.72	44.990	44.930	44.950
	55.64	55.33	56.82	55.973	55.793	55.833
	59.34	59.01	60.61	59.574	59.494	59.514
	65.21	64.84	66.65	65.436	65.376	65.376
	68.60		70.14	68.917	68.777	
	74.09	73.65	75.79	74.298	74.238	74.238
	77.30	77.90	79.11	77.519	77.459	77.459

of using electricity for the microwave equipment. From the perspective of synthesis, Tripathy and Bhattacharya [70] indicated that it is still an important challenge to synthesize mesoporous $MgAl_2O_4$ in a single step under rapid and economically viable approach. Their process required only 2 h to be completed by the flash pyrolysis route. Nevertheless, the process proposed in this manuscript might be seen as a competing alternative to produce $MgAl_2O_4$ spinel in a single step. The flow diagram of the solar process is presented in the Fig. 8.

It is important to remark that process proposed in this manuscript at laboratory scale required a maximum of 15 min for the process in the solar furnace. Even when the blending and crushing might be time consuming, the proposed route might represent a competitive alternative to produce the $MgAl_2O_4$ spinel.

Table 6 D-spacing of the hkl planes of the peaks in the X-ray diffraction pattern of solar $MgAl_2O_4$ spinel compared with those obtained by Paterson et al., (1991) [58] and some other spinels either found in the nature or synthesized in the laboratory

	hkl	$MgAl_2O_4$ -from Pein Pyit, Mogok, Myanmmar (natural) [58]	$MgAl_2O_4$ -from Bo Phloi, Kanchoutabori Province, Thailand (natural) [63]	$MgAl_2O_4$—(synthetic) [58]	$MgAl_2O_4$ -Canadian BPEFs	$MgAl_2O_4$ -Irish BPEFs	$MgAl_2O_4$ -Spanish BPEFs
d-spacing	111	4.6706		4.5830	4.6231	4.6423	4.6471
	220	2.8602	2.8743	2.8065	2.8426	2.8479	2.8496
	311	2.4392	2.4512	2.3934	2.4246	2.4297	2.4297
	222	2.3353		2.2915		2.3255	
	400	2.0224	2.0324	1.9845	2.0133	2.0159	2.0150
	422	1.6513	1.6595	1.6203	1.6442	1.6464	1.6453
	333	1.5569	1.5646	1.5277			
	511	1.5569	1.5646	1.5277	1.5506	1.5525	1.5520
	440	1.4301	1.4371	1.4033	1.4252	1.4263	1.4263
	531	1.3674		1.3418	1.3631	1.3638	
	620	1.2791	1.2854	1.2551	1.2756	1.2764	1.2764
	533	1.2337	1.2398	1.2105	1.2304	1.2312	1.2312

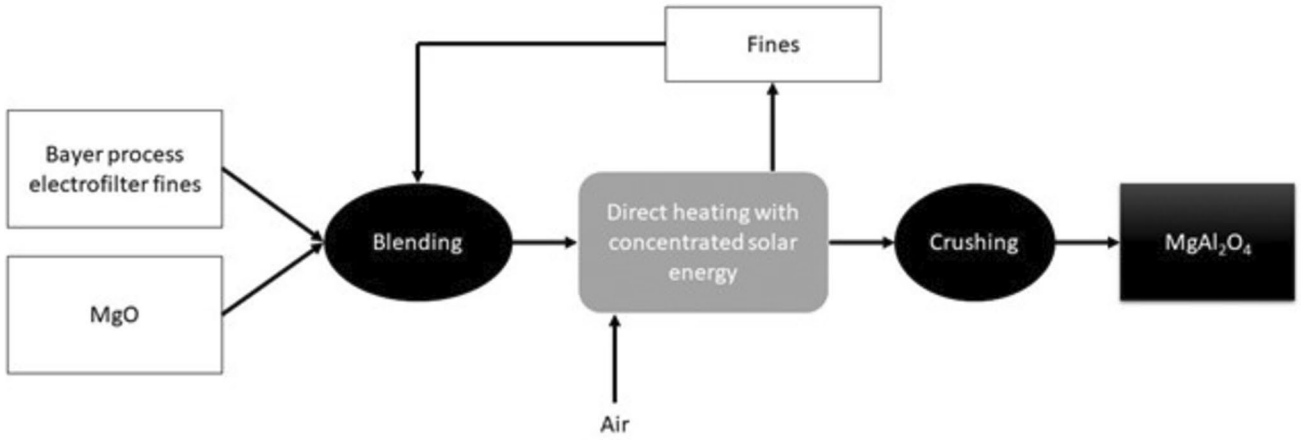

Fig. 8 Flow diagram of the solar process to produce $MgAl_2O_4$ spinel

The processing times might be significantly reduced as well as the productivity of the process might be increased in further steps aimed at the scalation of the process. The direct application of the solar energy, as a process like that conducted in electric furnaces where the heating is punctual, is a potential alternative to produce $MgAl_2O_4$ spinel although research conducted with other materials-processes might be potentially applied in this case. The production of lime by calcination of limestone and the thermal decomposition and reduction of zinc oxide with solar energy have been significantly studied using solar for the process [12]. The first investigations in this line were conducted by direct application of the solar beam to the samples in a laboratory scale but soon research acquired a greater dimension and investigators started to think about the increase of the productivity. Within this line, reactors are a key point and, therefore, have been significantly reviewed in the literature [71–73]. However, the importance of directly processing powders might be considered as one of the key points. Pilot plant scale studies have already validated the possibility of processing powders of limestone to produce lime, or reducing different metal oxides to obtain metal fuels, where the Paul Scherrer Institute has played an important role in the last 30 years [74]. Nevertheless, these indirectly heated reactors have never been applied in the synthesis $MgAl_2O_4$ spinel. Thus, the following investigations in this line should be oriented to the synthesis of the compound in the form of powders, which would reduce even more the processing times as the steps of blending and crushing may be eliminated. There is not too much information about the world production-consumption of $MgAl_2O_4$ spinel. Ganesh and collaborators indicated that the world consumption of spinel exceeded the 205,000 tons in 2004 [75]. This production, updated to current levels of consumption, might be easily covered with 10

solar factories considering that the conditions of production proposed by Meier and coauthors to produce lime (plant design of 25 MW_{th} operating for around 2700 h per year to produce 27,000 tons) [76] are applicable in the case of the $MgAl_2O_4$ spinel synthesis, although other researchers, as Purohit and researchers [77], increase the capacity of production (in this case for iron nuggets) to 200,000 tons/year. These technoeconomic studies, together with others reported in the review of Fernández-González [12] for different processes, suggest that the deployment of this technology at larger scale is only related with economic issues due to the lack of a plant operating for long periods of time under real conditions. Once validated in a real environment that it is possible to reach such capacities of production, plants to produce different materials will appear in countries with the suitable sun conditions.

Regarding the environmental issues, solar energy has a great potential in reducing carbon dioxide emissions. The energy demand required in the synthesis of the $MgAl_2O_4$ spinel was determined by means of the software HSC Chemistry 5.1. Calculations include heating from the room temperature (25 °C) to the synthesis temperature (assumed to be 1700 °C) and energy required for the formation of the compound. It is important to indicate that the formation of the spinel occurs partially through intermediate decomposition of the gibbsite with a Al_2O_3 to MgO molar ratio 1:1. Therefore, it is important to consider the gibbsite content in the thermodynamic calculations. Results are collected in the Table 7 for each residue of the aluminum industry, which indicates the energy required from the theoretical point of view.

Concentrated solar energy was directly applied to the sample. Power during the experiments was 900 W for a Direct Normalized Irradiation of around 1000 W/m^2 and a parabolic concentrator of 1.5 m in diameter with a concentration ratio of 15,000, a distance to the focal point of 65 cm, a maximum angle of incidence of 56° and a focal point of 1 cm in diameter. Therefore, the energy consumed during the experiments, which lasted for 5 min, is approximately 0.075 kWh to produce 2.4 g (31.25 kWh/kg, 112,500 kJ/kg). The efficiency of the process (η), defined as $\eta = (E_{Spinel}/E_{Total}) \cdot 100$, is < 5% in this case. In fact, Flamant and coauthors estimated that the energy conversion efficiency from the primary energy source to the useful energy beam reaches the 60% in the case solar furnaces [78]. It is necessary to remark at this point that there was not a strict control of the energy requirements in the process proposed in this manuscript as the objective was to demonstrate the feasibility of synthesizing the $MgAl_2O_4$ spinel.

The potential reduction in carbon dioxide emissions was calculated. The efficiency of the electric arc furnace was assumed to be in the range 40–75% [79], which would be the energy source replaced by the solar energy. The plant sizes were assumed to be of 1000, 5000 and 25,000 tons $MgAl_2O_4$ spinel per year, in agreement with the reference plant production sizes proposed by Meier and colleagues [76] for limestone calcination. Moreover, the carbon intensity of electricity in Spain in 2022 was 217 g CO_{2eq}/kWh, according to the Energy Institute Statistical Review of World Energy. Results of the carbon dioxide avoidance are collected in Table 8. It is possible to see that the utilization of concentrated solar energy in the production of $MgAl_2O_4$ spinel would promote a significant reduction in the greenhouse gas emissions and can contribute to the energy transition in the field of raw materials production for the manufacture of advanced ceramics.

Conclusions

The synthesis of ceramic materials still involves processes that generate significant quantities of greenhouse gases, thus contributing to the climate change. Within this context, solar energy, when it is adequately concentrated, emerges as a suitable alternative for high temperature processes. Therefore, this renewable energy source has been applied in the synthesis of $MgAl_2O_4$ spinel, where the source of alumina was a residue from the aluminum metallurgy called Bayer process electrofilter fines.

Table 7 Thermodynamic calculations for the formation of the $MgAl_2O_4$ spinel

Reaction		Energy demand (kJ/kg $MgAl_2O_4$)
$MgO + Al(OH)_3 \rightarrow MgAl_2O_4 + H_2O$		6047.7
$MgO + Al_2O_3 \rightarrow MgAl_2O_4$		1979.3
Energy demand (kJ/kg $MgAl_2O_4$)		
Canada	Ireland	Spain
3159.1	2569.2	2711.6

Table 8 Carbon dioxide emissions avoidance considering the data collected in Table 7

	Efficiency (%)	Canada	Ireland	Spain
Energy demand (theoretical) (kJ/kg)		3159.1	2569.2	2711.6
Energy demand (real) (kJ/kg)	40	7897.8	6423.0	6779.0
	75	4212.1	3425.6	3615.5
Plant size (t/y)		Energy demand (kWh)		
1000	40	2,193,835.1	1,784,168.1	1,883,057.1
	75	1,170,028.7	951,556.3	1,004,306.4
5000	40	10,969,175.4	8,920,840.5	9,415,285.3
	75	5,850,143.6	4,757,781.6	5,021,531.8
25,000	40	54,845,877.2	44,604,202.4	47,076,426.6
	75	29,250,717.8	23,788,907.9	25,107,659.0
Plant size (t/y)		CO_2 emissions avoidance (t/y)		
1000	40	476.1	387.2	408.6
	75	253.9	206.5	217.9
5000	40	2380.3	1935.8	2043.1
	75	1269.5	1032.4	1089.7
25,000	40	11,901.6	9679.1	10,215.6
	75	6347.4	5162.2	5448.4

The synthesis of the spinel was conducted in very short times, not exceeding the 5 min under the action of the solar beam. The solar spot was at temperatures clearly exceeding 1700 °C, as it was reported by mathematical simulations, which is sufficient for the formation of the compound. The formation of the $MgAl_2O_4$ spinel occurred partially through an intermediate process of decomposition of the gibbsite.

The fine particles of the residue together with the high heating rates and the water content produced certain mass losses that in a possible industrial process could be collected and sent back to the beginning of the treatment. Within this context, the direct application of the solar energy might be a technology that imitates the processes conducted in the electric arc furnaces in terms of direct application of the heat, although the processing of powders in indirectly solar heated furnaces might be a suitable alternative to directly process powder and reduce even more the processing times.

There is neither difference in terms of crystallinity nor phases when considering the three residues: Canada, Ireland, and Spain. The direct application of the solar radiation to the sample and the temperatures in excess to those required for the synthesis of the spinel hinder the possible influence of impurities in terms of reducing the synthesis temperature.

Three different scenarios were analyzed to evaluate the potential reduction in the carbon dioxide emissions. The values ranged from the 200 t/year in the case of small plants (1000 tons/year) to 12,000 t/year in the case of commercial plants (25,000 tons/year). This also translates into economics in terms of reducing the impact of the CO_2 emissions taxes.

Acknowledgements Daniel Fernández-González acknowledges the grant (Juan de la Cierva-Formación program) FJC2019-041139-I funded by the Ministerio de Ciencia e Innovación, Agencia Estatal de Investigación. Juan Piñuela Noval acknowledges the Programa "Severo Ochoa" of Grants for Research and Teaching of the Principality of Asturias for the funds received for the elaboration of the Ph. D. Thesis (Ref: BP20 041). We thank the PROMES-CNRS (PROcédés Matériaux et Energie Solaire- Centre National de la Recherche Scientifique) for providing access to its installations, the support of its scientific and technical staff, and the financial support of the SFERA-III project (Grant Agreement No 823802).

Declarations

Conflict of interest The authors have no competing interests to declare that are relevant to the content of this article.

Open Access This article is licensed under a Creative Commons Attribution 4.0 International License, which permits use, sharing, adaptation, distribution and reproduction in any medium or format, as long as you give appropriate credit to the original author(s) and the source, provide a link to the Creative Commons licence, and indicate if changes were made. The images or other third party material in this article are included in the article's Creative Commons licence, unless indicated otherwise in a credit line to the material. If material is not included in the article's Creative Commons licence and your intended use is not permitted by statutory regulation or exceeds the permitted use, you will need to obtain permission directly from the copyright holder. To view a copy of this licence, visit http://creativecommons.org/licenses/by/4.0/.

References

1. Pero-Sanz JA, Fernández-González D, Verdeja LF (2019) Structural materials. Properties and selection. Springer, Cham

2. Sancho JP, Verdeja LF, Ballester A (2000) Metalurgia extractiva. Síntesis, Madrid
3. Sancho J, Fernández Pérez B, Ayala J, Garcia, P, Verdeja LF (2009) The recycling of Bayer electrofilter fines for diverse applications, 1st Spanish National Conference on Advances in Materials Recycling and Eco – Energy, Madrid, 12–13, November 2009, S04–9, pp. 123–125.
4. Tutic E, Jovanovic M, Mujkanovic A (2016) Preparation of mullite ceramics from Bayer electrofilter fines and low kaolinite clay. Sci Sinter 48:247–257. https://doi.org/10.2298/SOS1602247T
5. Sancho-Gorostiaga J, Bernardo-Sánchez A, Sancho-Martínez JP, Fernández-González D, Verdeja LF (2021) Manufacture of a High Temperature Structural Insulator (HTSI) using electrofilter powders generated in the Bayer process. T Indian Ceram Soc 80:163–173. https://doi.org/10.1080/0371750X.2021.1915872
6. Okudan MD, Akcil A, Tuncuk A, Deveci H (2015) Recovery of gallium and aluminum from electrofilter dust of alumina calcination plant in Bayer process. Sep Sci Technol 50:2596–2605. https://doi.org/10.1080/01496395.2015.1062027
7. Ayala J, Fernández B (2015) Bayer electrofilter fines as potential Se(VI) adsorbents. JOM 67:2727–2732. https://doi.org/10.1007/s11837-015-1616-0
8. Sancho JP, Ayala J, García MP, Pérez B, Alonso D (2006) The sulfuric acid leaching of Bayer electrofilter fines: a practical kinetical approach. JOM 58:58–62. https://doi.org/10.1007/s11837-006-0055-3
9. Ayala JM, Sancho JP, García-Coque MP (2008) The Recycling of Electrofilter Fines to Produce Aluminum Sulfate. In: Proc. 2008 Global Symposium on Recycling, Waste Treatment and Clean Technology, REWAS 2008, Cancún, México, 2008: 419–426.
10. Sancho-Gorostiaga J, Bernardo-Sánchez A, Sancho-Martínez JP, Fernández-González D, Verdeja LF (2021) Study of copper fixation mechanisms on Bayer process electrostatic precipitator microparticles (BPEM) using ^{1}H and ^{27}Al NMR spectroscopy. J Water Process Eng 39:101872. https://doi.org/10.1016/j.jwpe.2020.101872
11. Fernández-González D, Ruiz-Bustinza I, González-Gasca C, Piñuela-Noval J, Mochón-Castaños J, Sancho-Gorostiaga J, Verdeja LF (2018) Concentrated solar energy applications in materials science and metallurgy. Sol Energy 170:520–540. https://doi.org/10.1016/j.solener.2018.05.065
12. Fernández-González D (2023) A state-of-the-art review on materials production and processing using solar energy. Mineral Proc Extr Metall Rev. https://doi.org/10.1080/08827508.2023.2243008
13. Fernández-González D, Prazuch J, Ruiz-Bustinza I, González-Gasca C, Piñuela-Noval J, Verdeja LF (2019) Transformations in the Si-O-Ca system: silicon-calcium via solar energy. Sol Energy 181:414–423. https://doi.org/10.1016/j.solener.2019.02.026
14. Fernández-González D, Prazuch J, Ruiz-Bustinza I, González-Gasca C, Piñuela-Noval J, Verdeja LF (2019) Transformations in the Mn-O-Si system using concentrated solar energy. Sol Energy 184:148–152. https://doi.org/10.1016/j.solener.2019.04.004
15. Fernández-González D, Prazuch J, Ruiz-Bustinza I, González-Gasca C, Piñuela-Noval J, Verdeja LF (2018) Solar synthesis of calcium aluminates. Sol Energy 171:658–666. https://doi.org/10.1016/j.solener.2018.07.012
16. Fernández-González D, Prazuch J, Ruiz-Bustinza I, González-Gasca C, Piñuela-Noval J, Verdeja LF (2018) Iron metallurgy via concentrated solar energy. Metals 8:873. https://doi.org/10.3390/met8110873
17. Fernández-González D, Piñuela-Noval J, Ruiz-Bustinza I, González-Gasca C, Gómez-Rodríguez C, García Quiñonez LV, Fernández A, Verdeja LF (2023) Solar dissociation of zirconium silicate sand: a clean alternative to obtain zirconium dioxide. J Clean Prod 420:138371. https://doi.org/10.1016/j.jclepro.2023.138371
18. Murray JP (1999) Aluminum production using high-temperature solar process heat. Sol Energy 66:133–142. https://doi.org/10.1016/S0038-092X(99)00011-0
19. Murray JP (1999) Aluminum-silicon carbothermal reduction using high-temperature solar process heat, 128th TMS Annual Meeting, San Diego, CA, 28 de February-4 de March, 1999 pp. 399–405.
20. Murray JP (2001) Solar production of aluminum by direct reduction: Preliminary results for two processes. J Sol Energ -T ASME 123:125–132. https://doi.org/10.1115/1.1351809
21. Kruesi M, Galvez ME, Halmann M, Steinfeld A (2011) Solar aluminum production by vacuum carbothermal reduction of alumina-Thermodynamic and experimental analyses. Metall Mater Trans B 42B:254–260. https://doi.org/10.1007/s11663-010-9461-6
22. Vishnevetsky I, Ben-Zvi R, Epstein M, Barak S, Rubin R (2013) Solar carboreduction of alumina under vacuum. JOM 65:1721–1732. https://doi.org/10.1007/s11837-013-0777-y
23. Puig J, Balat-Pichelin M (2016) Production of metallic nanopowders (Mg, Al) by solar carbothermal reduction of their oxides at low pressure. J Mag Alloy 4:140–150. https://doi.org/10.1016/j.jma.2016.05.003
24. Puig J, Balat-Pichelin M (2020) Experimental carbothermal reduction of Al_2O_3 at low pressure using concentrated solar energy. J Sustain Metall 6:161–173. https://doi.org/10.1007/s40831-020-00266-7
25. Lytvynenko YM (2013) Obtaining aluminum by the electrolysis with the solar radiation using. Appl Sol Energy 49:4–6. https://doi.org/10.3103/S0003701X13010088
26. Davis D, Müller F, Saw WL, Steinfeld A, Nathan G (2017) Solar-driven alumina calcination for CO_2 mitigation and improved product quality. Green Chem 19:2992–3005. https://doi.org/10.1039/C7GC00585G
27. Kakosimos KE, Fhatima N, Al-Rawashdeh M (2022) Alrawashdeh M (2022) Conversion of boehmite to higher alumina phases by direct irradiation with concentrated light: numerical modelling and experimental verification. AIP Conf Proc 2445:130005
28. Fernández-González D, Prazuch J, Ruiz-Bustinza I et al (2021) Recovery of copper and magnetite from copper slag using concentrated solar power (CSP). Metals 11:1032. https://doi.org/10.3390/met11071032
29. Fernández-González D, Prazuch J, Ruiz-Bustinza I, González-Gasca C, Gómez-Rodríguez C, Verdeja LF (2019) The treatment of basic oxygen furnace (BOF) slag with concentrated solar energy. Sol Energy 180:372–382. https://doi.org/10.3390/met11071032
30. Binner P, Plötz F, Funken KH, Knoche KF (1995) The evaluation of a solar process for the high temperature treatment of hazardous wastes with solar energy. In: Proceedings of 7th Int. Symp. Solar Thermal Conc. Technol., Moscow, Russia, 1994: 497–508.
31. Funken KH, Pohlmann B, Lüpfert E, Dominik R (1999) Application of concentrated solar radiation to high temperature detoxification and recycling processes of hazardous wastes. Sol Energy 65:25–31. https://doi.org/10.1016/S0038-092X(98)00089-9
32. Navarro A, Cañadas I, Martinez D, Rodríguez J, Mendoza JL (2009) Application of solar thermal desorption to remediation of mercury-contaminated soils. Sol Energy 83:1405–1414. https://doi.org/10.1016/j.solener.2009.03.013
33. Navarro A, Cañadas I, Rodríguez J, Martinez D (2012) Leaching characteristics of mercury mine wastes before and after solar thermal desorption. Environ Eng Sci 29:915–928. https://doi.org/10.1089/ees.2010.0017
34. Navarro A, Cardellach E, Cañadas I, Rodríguez J (2013) Solar thermal vitrification of mining contaminated soils. Int J Miner Process 119:65–74. https://doi.org/10.1016/j.minpro.2012.12.002
35. Navarro A, Cañadas I, Rodríguez J (2014) Thermal treatment of mercury mine wastes using a rotary solar kiln. Minerals 4:37–51. https://doi.org/10.3390/min4010037

36. Schaffner B, Hoffelner W, Sun H, Steinfeld A (2000) Recycling of hazardous solid waste material using high-temperature solar process heat. 1 thermodynamic analysis. Environ Sci Technol 34:4177–4184. https://doi.org/10.1021/es0000495
37. Schaffner B, Meier A, Wuillemin D, Hoffelner W, Steinfeld A (2003) Recycling of hazardous solid waste material using high-temperature solar process heat. 2. Reactor design and experimentation. Environ Sci Technol 37:165–170. https://doi.org/10.1021/es020056o
38. Tzouganatos N, Matter R, Wieckert C, Antrekowitsch J, Gamroth M, Steinfeld A (2013) Thermal recycling of waelsz oxide using concentrated solar energy. JOM 65:1733–1743. https://doi.org/10.1007/s11837-013-0778-x
39. Funken KH, Roeb M, Schwarzboezl P, Warnecke H (2001) Aluminum remelting using directly solar-heated rotary kilns. J Sol Energ-T ASME 123(2):117–124. https://doi.org/10.1115/1.1355242
40. Roeb M, Monnerie N, Schäfer R, Rohner N (2003) Thermal treatment of industrial residues using concentrated sunlight, Int. Symp. on Recycling and Reuse of Waste Materials, Dundee, Scotland, UK, 9-11 Sep. 2003
41. Puttkamer MNV, Roeb M, Tescari S, de Oliveira L, Breuer S, Sattler C (2016) Solar aluminum recycling in a directly heated rotary kiln. REWAS 2016:233–240
42. Demirtas C, Ozcan AK (2021) The experimental thermal analysis of aluminum metal melting with concentrated solar energy. Sol Energ Mat Sol C 222:11094010. https://doi.org/10.1016/j.solmat.2020.110940
43. Padilla I, López-Delgado A, López-Andrés S, Álvarez M, Galindo R, Vázquez-Vaamonde AJ (2014) The application of thermal solar energy to high temperature processes: case study of the synthesis of alumina from boehmite. Sci World J 2014:825745. https://doi.org/10.1155/2014/825745
44. Padilla I, Romero M, Robla JI, López-Delgado A (2021) Waste and solar energy: an eco-friendly way for glass melting. ChemEngineering 5:16. https://doi.org/10.3390/chemengineering5020016
45. Ganesh I (2013) A review on magnesium aluminate ($MgAl_2O_4$) spinel: synthesis, processing and applications. Int Mater Rev 58:63–112. https://doi.org/10.1179/1743280412Y.0000000001
46. Ping LR, Azad AM, Dung TW (2001) Magnesium aluminate ($MgAl_2O_4$) spinel produced via self-heat-sustained (SHS) technique. Mater Res Bull 36:1417–1430. https://doi.org/10.1016/S0025-5408(01)00622-5
47. Li H, Wei HY, Cui Y, Sang RL, Bu JL, Wei YN, Lin J, Zhao JH (2017) Synthesis and characterisation of $MgAl_2O_4$ spinel nanopowders via nonhydrolytic sol–gel route. J Ceram Soc Jpn 125:100–104. https://doi.org/10.2109/jcersj2.16297
48. Figueredo GP, Carvalho AFM, Medeiros RLBA, Silva FM, de Macedo HP, de Freitas Melo MA, de Araujo Melo DM (2017) Synthesis of $MgAl_2O_4$ by gelatin method: effect of temperature and time of calcination in crystalline structure. Mat Res 20:254–259. https://doi.org/10.1590/1980-5373-MR-2017-0105
49. Nuernberg GDB, Foletto EL, Probst LFD, Campos CEM, Carreño NLV, Moreira MA (2012) A novel synthetic route for magnesium aluminate ($MgAl_2O_4$) particles using metal–chitosan complexation method. Chem Eng J 193–194:211–214. https://doi.org/10.1016/j.cej.2012.04.054
50. Miroliaee A, Salehirad A, Rezvani AR (2015) Ion-pair complex precursor approach to fabricate high surface area nanopowders of $MgAl_2O_4$ spinel. Mater Chem Phys 151:312–317. https://doi.org/10.1016/j.matchemphys.2014.11.072
51. Zhang X (2009) Hydrothermal synthesis and catalytic performance of high-surface-area mesoporous nanocrystallite $MgAl_2O_4$ as catalyst support. Mater Chem Phys 116:415–420. https://doi.org/10.1016/j.matchemphys.2009.04.012
52. Kong LB, Ma J, Huang H (2002) $MgAl_2O_4$ spinel phase derived from oxide mixture activated by a high-energy ball milling process. Mater Lett 56:238–243. https://doi.org/10.1016/S0167-577X(02)00447-0
53. Ganesh I, Johnson R, Rao GVN, Mahajan YR, Madavendra SS, Reddy BM (2005) Microwave-assisted combustion synthesis of nanocrystalline $MgAl_2O_4$ spinel powder. Ceram Int 31:67–74. https://doi.org/10.1016/j.ceramint.2004.03.036
54. Pacurariu C, Lazau I, Ecsedi Z, Lazau R, Barvinschi P, Marginean G (2007) New synthesis methods of $MgAl_2O_4$ spinel. J Eur Ceram Soc 27:707–710. https://doi.org/10.1016/j.jeurceramsoc.2006.04.050
55. Troia A, Pavese M, Geobaldo F (2009) Sonochemical preparation of high surface area $MgAl_2O_4$ spinel. Ultrason Sonochem 16:136–140. https://doi.org/10.1016/j.ultsonch.2008.06.001
56. Suyama Y, Kato A (1982) Characterization and sintering of Mg-Al spinel prepared by spray-pyrolysis technique. Ceram Int 8:17–21. https://doi.org/10.1016/0272-8842(82)90010-4
57. Montouillout V, Massiot D, Douy A, Coutures JP (2004) Characterization of $MgAl_2O_4$ precursor powders prepared by aqueous route. J Am Ceram Soc 82:3299–3304. https://doi.org/10.1111/j.1151-2916.1999.tb02243.x
58. Sarkar R, Banerjee G (1999) Effect of compositional variation and fineness on the densification of $MgO–Al_2O_3$ compacts. J Eur Ceram Soc 19:2893–2899. https://doi.org/10.1016/S0955-2219(99)00078-3
59. Tong ZF, Qiao JL, Jiang XY (2017) Kinetics of Na_2O evaporation from $CaO–Al_2O_3–SiO_2–MgO–TiO_2–Na_2O$ slags. Ironmak Steelmak 44:237–245. https://doi.org/10.1080/03019233.2016.1210354
60. Meier A, Bonaldi E, Cella GM, Lipinski W, Wuillemin D (2006) Solar chemical reactor technology for industrial production of lime. Sol Energ 80:1355–1362. https://doi.org/10.1016/j.solener.2005.05.017
61. Hauter P, Moeller S, Palumbo R, Steinfeld A (1999) The production of zinc by thermal dissociation of zinc oxide—solar chemical reactor design. Sol Energ 67:161–167. https://doi.org/10.1016/S0038-092X(00)00037-2
62. Peterson RC, Lager GA, Hitterman RL (1991) A time-of-flight neutron powder diffraction study of $MgAl_2O_4$ at temperatures up to 1273 K. Am Mineral 76:1455–1458
63. Lucchesi S, Russo U, Della Giusta A (1997) Crystal chemistry and cation distribution in some Mn-rich natural and synthetic spinel. Eur J Mineral 9:31–42
64. Pei LZ, Yin WY, Wang JF, Chen J, Fan CG, Zhang QF (2010) Low temperature synthesis of magnesium oxide and spinel powders by a sol-gel process. Mater Res 13:339–343. https://doi.org/10.1590/S1516-14392010000300010
65. Sanjabi S, Obeydavi A (2015) Synthesis and characterization of nanocrystalline $MgAl_2O_4$ spinel via modified sol–gel method. J Alloy Compd 645:535–540. https://doi.org/10.1016/j.jallcom.2015.05.107
66. Meng J, Chen W, Zhao J, Liu L (2017) Study of the high-temperature synthesis of $MgAl_2O_4$ spinel refractory raw materials from chromium slag. High Temp Mater Proc 37:581–586. https://doi.org/10.1515/htmp-2016-0254
67. Bocanegra SA, Ballarini AD, Scelza OA, de Miguel SR (2008) The influence of the synthesis routes of $MgAl_2O_4$ on its properties and behavior as support of dehydrogenation catalysts. Mater Chem Phys 111:534–541. https://doi.org/10.1016/j.matchemphys.2008.05.002
68. Bai J, Liu J, Li C, Li G, Du Q (2011) Mixture of fuels approach for solution combustion synthesis of nanoscale $MgAl_2O_4$ powders. Adv Powder Technol 22:72–76. https://doi.org/10.1016/j.apt.2010.03.013

69. Lee PY, Suematsu H, Yano T, Yatsui K (2006) Synthesis and characterization of nanocrystalline $MgAl_2O_4$ spinel by polymerized complex method. J Nanopart Res 8:911–917. https://doi.org/10.1007/s11051-005-9055-4
70. Tripathy S, Bhattacharya D (2013) Rapid synthesis and characterization of mesoporous nanocrystalline $MgAl_2O_4$ via flash pyrolysis route. J Asian Ceram Soc 1:328–332. https://doi.org/10.1016/j.jascer.2013.08.006
71. Abbas SA, Eidan AA, Al Sahlani A (2022) Solar reactor review. Solar reactor review. Int J Heat Technol 40(3):671–84. https://doi.org/10.18280/ijht.400303
72. Ekman BM, Brooks G, Rhamdhani MA (2014) A review: Solar thermal reactors for materials production (Chapter 1). In: Wang C, de Bakker J, Belt CK, Jha A, Neelameggham NR, Pati S, Prentice LH, Tranell G, Brinkman KS (eds) Energy technology 2014: Carbon dioxide management and other technologies. John Wiley, London. https://doi.org/10.1002/9781118888735.ch1
73. Guerra-Rosa L (2019) Solar heat for materials processing: a review on recent achievements and a prospect on future trends. Chemengineering 3(4):83. https://doi.org/10.3390/chemengineering3040083
74. Koepf E, Alxneit I, Wieckert C, Meier A (2017) A review of high temperature solar driven reactor technology: 25 years of experience in research and development at the Paul Scherrer Institute. Appl Energ 188:620–651. https://doi.org/10.1016/j.apenergy.2016.11.088
75. Ganesh I, Srinivas B, Johnson R, Saha BP, Mahajan YR (2004) Microwave assisted solid state reaction synthesis of $MgAl_2O_4$ spinel powders. J Eur Ceram Soc 24:201–207. https://doi.org/10.1016/S0955-2219(03)00602-2
76. Meier A, Gremaud N, Steinfeld A (2005) Economic evaluation of the industrial solar production of lime. Energ Convers Manage 46:905–926. https://doi.org/10.1016/j.enconman.2004.06.005
77. Purohit S, Ekman B, Mejias R, Brooks G, Rhamdhani MA (2018) Solar processing of composite iron ore pellets: preliminary assessments. J Clean Prod 205:1017–1028. https://doi.org/10.1016/j.jclepro.2018.09.112
78. Flamant G, Ferriere A, Laplaze D, Monty C (1999) Solar processing of materials: opportunities and new frontiers. Sol Energ 66:117–132. https://doi.org/10.1016/S0038-092X(98)00112-1
79. Kirschen M, Risonarta V, Pfeifer H (2009) Energy efficiency and the influence of gas burners to the energy related carbon dioxide emissions of electric arc furnaces in steel industry. Energy 34:1065–1072. https://doi.org/10.1016/j.energy.2009.04.015

Publisher's Note Springer Nature remains neutral with regard to jurisdictional claims in published maps and institutional affiliations.